

Structuring of high latitude plasma patches with variable drive

N. A. Gondarenko and P. N. Guzdar

IREAP, University of Maryland, College Park, Maryland, USA

J. J. Sojka and M. David

CASS, Utah State University, Logan, Utah, USA

Received 10 October 2002; revised 11 December 2002; accepted 27 December 2002; published 21 February 2003.

[1] Three-dimensional nonlinear simulations of the structuring of high-latitude patches with variable drive demonstrate the role of the gradient drift instability as the primary operative structuring mechanism. In this letter we show that by introducing a variable convective $E \times B$ drive obtained from the ionosphere module of a global MHD code simulation of a real substorm [Sojka *et al.*, 1997], the nature of the structuring is strongly influenced by the drive. In fact, due to occasional reversal of the direction of the convection, the structuring from the gradient-drift instability takes place on both edges of the patch. Using different ion-neutral collisionality to account for the seasonal or solar cycle variability of the ionosphere, the four categories of structured patches identified by Kivanç and Heelis [1997] have been simulated. **INDEX TERMS:** 2439 Ionosphere: Ionospheric irregularities; 2437 Ionosphere: Ionospheric dynamics; 2463 Ionosphere: Plasma convection; 2407 Ionosphere: Auroral ionosphere (2704); 2435 Ionosphere: Ionospheric disturbances. **Citation:** Gondarenko, N. A., P. N. Guzdar, J. J. Sojka, and M. David, Structuring of high latitude plasma patches with variable drive, *Geophys. Res. Lett.*, 30(4), 1165, doi:10.1029/2002GL016437, 2003.

1. Introduction

[2] The high latitude ionosphere has very variable large scale plasma structures referred to as patches and auroral blobs with scale sizes of hundreds of kilometers and densities of two to ten times the background density. The observation of these interesting plasma structures have been reviewed by Tsunoda [1988]; Crowley [1996]; and Basu and Valladares [1999]. Embedded in these large scale structures are mesoscale irregularities in the range of 0.1 km to tens of kilometers. Observations [Weber *et al.*, 1986; Basu *et al.*, 1994] and modeling studies [Sojka *et al.*, 1993; Basu *et al.*, 1995] indicate that the patches convect to long distances, ~ 3000 km, [Weber *et al.*, 1986] for long periods of time (hours) retaining their distinct identity and integrity.

[3] The observational studies that have primarily focused on the mesoscale structures have been reported by Weber *et al.* [1984, 1986]; Basu *et al.* [1990], and more recently by Kivanç and Heelis [1997, 1998]. All these investigations use satellite data to characterize the density and velocity or electric field irregularities. Besides the investigation of the spectral characteristics of the irregularities, one of the central issues is to ascertain whether the mesoscale structuring arises from naturally occurring plasma instabilities like

the gradient drift instability or due to complicated passive scalar convection of the density. The variety of observed characteristics in these patches leads to this uncertainty. One expects that if the gradient drift instability was operative, then the instabilities would occur preferentially on one side, namely the trailing edge of the patch and also that the instability remain confined to the steep edges. Thus there would be a significant asymmetry between the trailing edge and leading edge of the patches. On the other hand, if passive scalar convection of the density in existing turbulent flow fields was the operative mechanism for the generation of the density irregularities, there would be no preferential asymmetry between the two edges of the patch. In fact Kivanç and Heelis [1997] with DE2 satellite data carefully studied 18 patches identified by the Coley-Heelis algorithm [Coley and Heelis, 1995]. The study was for noon-midnight passes of the DE2 satellite. They concluded that there are four groups that the patches fall into based on their structuring characteristics. They are (a) fully structured patches, (b) patches with structure only on the edges, (c) patches with only one structured edge, and (d) unstructured patches. Furthermore the majority of the patches belonged to the first two categories. The last two groups had only one example each from the 18 patches investigated. It is precisely this variability, which contributes significantly to the overall ambiguity in interpreting the cause of the structuring.

[4] In a series of papers [Guzdar *et al.*, 1998; Gondarenko and Guzdar, 1999, 2001, 2002], we have reported three-dimensional (3-D) nonlinear simulations, first for the collisional gradient-drift instability (GDI), followed by those with ion inertial effects, to model the mesoscale structures in plasma patches. For the purely collisional case, the basic structuring occurred transverse to the direction of the magnetic field and to the direction of the ambient density gradient in long elongated “fingers”. The parallel dynamics of the electrons was responsible for slowing down the structuring process [Chaturvedi and Huba, 1987]. However, with the inclusion of the nonlinear ion inertial effects, secondary instabilities were possible. The highly elongated vortices associated with fingers were unstable to the Kelvin-Helmholtz instability, which subsequently broke them into smaller vortices. These small scale vortices were then prone to a tertiary instability, which generated shear flow transverse to the magnetic field and to the direction of the ambient density gradient [Gondarenko and Guzdar, 1999, 2001, 2002]. Thus the final nonlinear state consists of density and potential fluctuation embedded in multiple shear layers on the scale-size of the irregularities. The overall consequence of this hierarchy of instabilities was

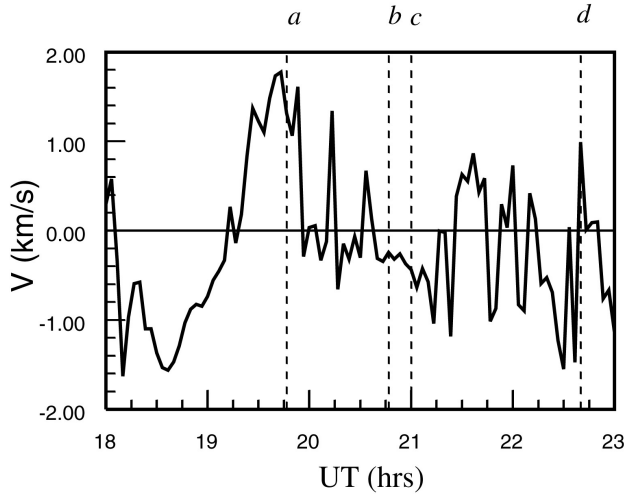


Figure 1. Convection velocity as a function of time (UT).

to significantly slow down the structuring process and allow the patch to survive for many hours.

[5] In all these studies we had assumed that the drive (a combination of $E \times B$ and neutral wind velocity), which is responsible for the primary gradient drift instability, was a constant in time. However, the convection drive can be highly variable over the time period of a few hours. Since the gradient drift instability, which depends on the magnitude and direction of the flow velocity, is the primary instability that causes the structuring, the temporal development is strongly influenced by the temporal variability of the flow. In fact, since the gradient drift instability occurs on the trailing edge and observations indicate that on many occasions the structuring also occurs on the leading edge, it has been suggested that other instabilities (such as fluid interchange instabilities [Keskinen and Ossakow, 1983]) besides the gradient drift were responsible for the structuring of plasma patches. Our earlier work shows that the initial instability does develop on the trailing edge, but in its full nonlinear development it penetrates through the patch and reaches the leading edge. However, if the variable drive changes the direction of the convection, structuring can occur on both sides.

[6] In this letter we present our first simulations with a variable drive. The representative convection velocity was obtained from the ionospheric module of the NRL global MHD code [Fedder and Lyon, 1995; Fedder et al., 1995]. These simulations were performed for a real event and the $E \times B$ velocity is shown in Figure 1. The magnitude of the velocity can be as large as 1.5 km/s. Besides the variation in the magnitude of the velocity, the plot shows that direction of the flow velocity changes from the anti-sunward direction at 19:30 UT to the sunward direction. The sunward flow is sustained for about 45 minutes after which the flow velocity makes a number of excursions from sunward to anti-sunward directions in a period of three hours.

2. Simulation Results

[7] The basic geometry for the high latitude plasma patch used in our simulations is the following. The Earth's field lines are vertical and aligned with the z axis. The $-x$ axis points anti-sunward, and the y axis is orthogonal to the x

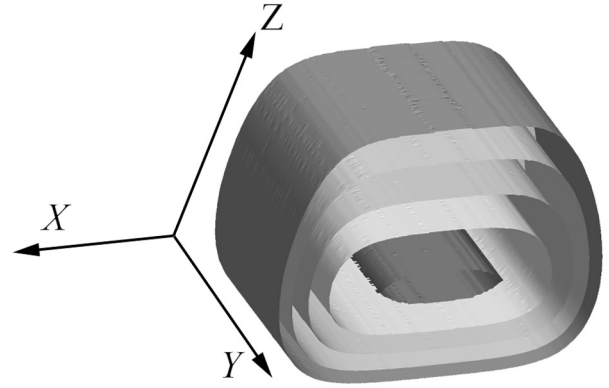


Figure 2. Five density isosurfaces of the initial patch.

and z directions. For these simulations we have considered the whole patch. The size of the box in the x and y directions are 200 km and 12.56 km respectively. The density profile in x is a tanh function to model a localized patch and for the z dependence we have used the Chapman function. The size of the patch in the z direction is 1100 km. The peak density is assumed to be twice the background density at the height of 417 km of the F peak. The number of grid points used in the simulation are 260, 132, 51 in the x , y , and z directions, respectively. Five equally spaced isosurfaces of the initial patch density are shown in Figure 2, with the innermost surface representing the highest density and the outer the lowest. The choice of the ion-neutral collision frequency is such that the plasma is strongly collisional at F peak. This was a representative plasma collisionality during the solar maximum period. A second run, with the same convection velocity but with the ion-neutral collisionality at the F peak being about hundred times smaller to represent solar minimum conditions, was also studied.

[8] In Figures 3a–3c we show the evolution of the density isosurfaces at four instant of times indicated by

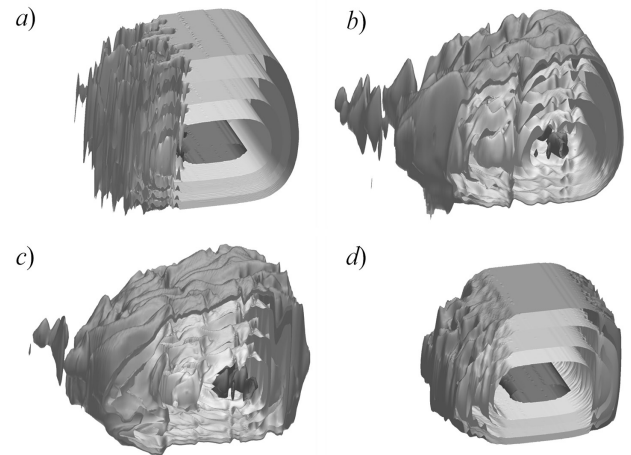


Figure 3. Evolution of the density isosurfaces at the instant of times indicated by the dashed lines in Figure 1 at (a) $t = 19:47$ UT, (b) $t = 20:47$ UT, and (c) $t = 21:00$ UT for the solar maximum case, and $t = 22:40$ UT for the solar minimum case.

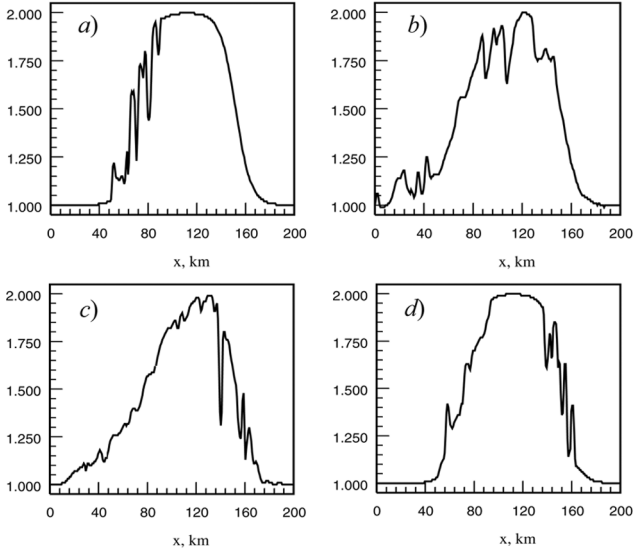


Figure 4. Density (at the F peak in z and an arbitrary point in y) versus x at four instant of times in Figures 3a–3d.

the dashed lines in Figure 1 at (a) $t = 19:47$ UT, (b) $t = 20:47$ UT, and (c) $t = 21:00$ UT for the solar maximum case while Figure 3d at $t = 22:40$ UT is for the solar minimum case. For the simulation run depicted in Figures 3a–3c, the unperturbed patch was launched at 19:20 UT just about the time the direction of convection became sunward. In the very early phase at $t = 19:47$ UT the initial gradient drift instability causes very fine scale structuring on the night-side of the patch. Since the convection velocity is about 1.5 km/s the present state of development of the irregularities occurs in tens of minutes. An hour later at $t = 20:47$ UT, just after the flow velocity has reversed, Figure 3b shows that the structuring has penetrated almost through the entire patch. Also, the irregularities have larger scales compared to the early phase shown in Figure 3a, since secondary instabilities and inverse cascade have taken place [Gondarenko and Guzdar, 2001].

[9] Another interesting feature evident in the structuring is that the irregularities, which occur on the trailing edge, tend to “anomalously” transport the density so that the size of the trailing edge gets extended. Since the instability feeds off the density gradient, the nonlinear evolution reduces the average density scalelength, thereby causing further reduction in the strength of the instability. Up to this point the basic characteristic of the structuring is very similar to the case with a constant drive. Thus for most cases even if the drive is variable, but is predominantly in one direction (for most cases it is anti-sunward), the structuring will penetrate through the whole patch all the way to the stable side. It is assumed that initially the patch has similar scale-lengths on the leading and trailing edges. In this case, one clear signature of the gradient drift instability would be that the trailing edge would have a longer scalelength compared to the leading edge even if the instability penetrates through the entire patch. Thus for most of the times one should observe fully structured patches with the trailing edge more extended with a larger density scalelength than the leading edge.

[10] The importance of the flow reversal is evident in Figure 3c where we show the isosurfaces at $t = 21:00$ UT.

Figure 1 shows that the direction of the flow had reversed to the anti-sunward direction at $t = 20:30$ UT and remained so till 21:30 UT. Thus the trailing edge is now on the right side of the patch. There are two interesting features that are evident in this plot. The first notable point is that now the structuring is dominantly on the right trailing edge. However, the fluctuation levels on the current leading edge have significantly reduced. This is because of the perturbations on the trailing edge develop initially with a growth rate V/L_n , where V is the convection velocity, and L_n is the density gradient scale length, while those on the leading edge damp at the same rate. However, since the scalelengths are now different on the two edges, the damping rate is slower on the current leading edge compared to the growth on the trailing edge. Thus the structuring appears to be on one edge at this instant of time. At an even later instant of time at $t = 23:00$ UT, the patch appears to be unstructured due to the many reversals in the direction of flow during the entire duration of the simulation period from $t = 19:33$ UT to $t = 23:00$ UT. Hence, we see that just within one single event with a variable drive having reversals of the flow direction, three of the four different patch morphologies categorized by Kivanc and Heelis [1997] have been observed in the simulations. However, for most cases that we have simulated, with the velocity drive mostly unidirectional, the fully structured patch is the most prevalent, and there is clear asymmetry in the scale size of the trailing edge compared to the leading edge. The trailing edge is longer due to the turbulence driven transport. This asymmetry is typically within a factor of two. Coley and Heelis [1998] have examined the density gradients of the patch edges and have concluded that the leading edge gradient was about 67% larger than the trailing edge.

[11] The fourth category, though rare, with both structured edges and unstructured core, was not observed in these simulations. However, one of the major sources of seasonal or solar cycle variability is the ion-neutral collisionality of the ionospheric plasma. The case discussed till now was representative of high collisionality, in which the ion-neutral collision frequency at F peak was significantly larger than the initial growth rate of the gradient drift instability. We ran a second case with the same flow velocity history as in Figure 1, but with ion-neutral collisionality at the F peak comparable to the initial growth rate of the gradient drift instability. For this case the initial patch was launched at $t = 18:00$ UT, and in Figure 3d is shown the

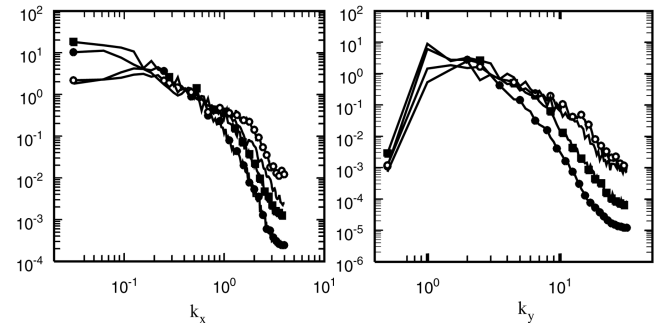


Figure 5. Density power spectra at four instant of times in Figures 3a–3d versus (a) k_x and (b) k_y .

state of the structuring 4 3/4 hours later. Since the growth rate for the instability is strongly reduced for this case, the nonlinear development of the irregularities progresses very slowly. The initial structuring which begins on the right trailing edge cannot penetrate into the patch on the time scale of hours. The reversal of the flow direction at $t = 19:15$ UT causes the structuring to start on the left side trailing edge. Although there is stabilization occurring on the left side of the patch (now the leading side), the damping is too weak to completely suppress the fluctuations. Thus, Figure 3d shows that the patch has structuring only on the two edges and the core of the patch is unstructured. One can observe that there is no general asymmetry in the density profile in this case.

[12] In Figures 4a–4b we show lineouts of the density (at the F peak and an arbitrary point in y) as a function of x at (a) $t = 19:47$ UT, (b) $t = 20:47$ UT, and (c) $t = 21:00$ UT for the high collisionality case, and Figure 3d at $t = 22:40$ UT for the low collisionality case. In Figure 4a the lineout shows the highly structured trailing edge. Figure 4b shows the penetration of the structuring through the patch. The reversal of the flow at $t = 21:14$ UT causes the primary structuring to occur on the right side of the patch as shown in Figure 4c at $t = 21:00$ UT. The suppression of the irregularities on the current leading edge (left side) is very clearly seen in this lineout. Finally, for the low collisionality case, the structuring localized to the both edge regions is evident in the Figure 4b at $t = 23:00$ UT.

[13] This large variability in the nature of the structuring can also be reflected in the power spectra. In Figures 5a and 5b are shown the power spectra of the density as a function of k_x and k_y , respectively, for the four instants of time as in Figures 3 and 4, namely, $t = 19:47$ UT (solid line), $t = 20:47$ UT (solid-circle line), and $t = 21:00$ UT (solid-box line) for the high collisionality case, and $t = 22:40$ UT (open-circle line) for the low collisionality case. Though the present simulations are restricted in terms of the spectral range, there is a clear indication that the spectral index for the irregularities can vary compared to the k^{-2} observed at late times in our earlier constant drive simulations. Thus, the large range in the spectral index histograms shown by Kivanc and Heelis [1998] is to be expected.

[14] In conclusion, we have demonstrated that variable drive can strongly influence the structuring characteristics of plasma patches, and with different ion-neutral collisionality due to seasonal and solar cycle variability, our simulations can readily account for the broad classification of patches into four distinct categories identified by Kivanc and Heelis [1997]. The large variability in the observed features, which on the surface casts doubts about the role of the gradient drift instability as the primary operative structuring mechanism, can be readily explained by taking into account the temporal character of the convection velocity and the variable ionospheric collisionality. When these two effects are incorporated into the nonlinear simulations, the observed features are consistent with the nonlinear evolution of a primary gradient drift instability,

and subsequent secondary Kelvin-Helmholtz and tertiary shear-flow instabilities.

[15] **Acknowledgments.** We acknowledge useful discussions with Drs. Sunanda Basu, Shantimay Basu, Rod Heelis and Todd Pedersen. This research was supported by the NSF under grant ATM-0122874. Also, this research was supported by NASA grant NAG5-11880 and NSF grant ATM-0000171 to Utah State University.

References

- Basu, Su., and C. Valladares, Global aspects of plasma structures, *J. Atmos. Sol-Terr. Phys.*, **61**, 127, 1999.
- Basu, Su., et al., Plasma structuring by the gradient drift instability at high latitudes and comparison with velocity shear driven processes, *J. Geophys. Res.*, **95**, 7799, 1990.
- Basu, S., et al., Irregularity structures in the cusp/cleft and polar cap regions, *Radio Sci.*, **29**, 195, 1994.
- Basu, S., et al., Macroscale modeling and mesoscale observations of plasma density structures in the polar cap, *Geophys. Res. Lett.*, **22**, 881, 1995.
- Chaturvedi, P. K., and J. D. Huba, The interchange instability in high latitude plasma blobs, *J. Geophys. Res.*, **92**, 3357, 1987.
- Coley, W. R., and R. A. Heelis, Adaptive identification and characterization of polar ionization patches, *J. Geophys. Res.*, **100**, 23,819, 1995.
- Coley, W. R., and R. A. Heelis, Structure and occurrence of polar ionization patches, *J. Geophys. Res.*, **103**, 2201, 1998.
- Crowley, G., Critical Review on Ionospheric Patches and Blobs, *The Review of Radio Sci.*, Oxford University Press, 1, 1996.
- Fedder, J. A., and J. G. Lyon, The Earth's magnetosphere is 165 RE long: Self-consistent currents, convection, magnetospheric structure, and processes for northward interplanetary magnetic field, *J. Geophys. Res.*, **100**, 3623, 1995.
- Fedder, J. A., J. G. Lyon, S. P. Slinker, and C. M. Mobarry, Topological structure of the magnetotail as a function of interplanetary magnetic field direction, *J. Geophys. Res.*, **100**, 3613, 1995.
- Gondarenko, N. A., and P. N. Guzdar, Gradient drift instability in high latitude plasma patches: Ion inertial effects, *Geophys. Res. Lett.*, **36**, 3345, 1999.
- Gondarenko, N. A., and P. N. Guzdar, Three-dimensional structuring characteristics of high-latitude plasma patches, *J. Geophys. Res.*, **106**, 24,611, 2001.
- Gondarenko, N. A., and P. N. Guzdar, Structure of Turbulent Irregularities in High-Latitude Plasma Patches-3D Nonlinear Simulations, to appear in AGU Monograph on Storm-Substorm Relationship, 2002.
- Guzdar, P. N., et al., Three-dimensional nonlinear simulations of the gradient drift instability in the high latitude ionosphere, *Radio Sci.*, **33**, 1901, 1998.
- Keskinen, M. J., and S. L. Ossakow, Theories of high latitude irregularities: A review, *Radio Sci.*, **18**, 1077, 1983.
- Kivanc, Ö., and R. A. Heelis, Structures in ionospheric number density and velocity associated with polar cap ionization patches, *J. Geophys. Res.*, **102**, 307, 1997.
- Kivanc, Ö., and R. A. Heelis, Spatial distribution of ionospheric plasma and field structures in the high-latitude F region, *J. Geophys. Res.*, **103**, 6955, 1998.
- Sojka, J. J., et al., Modeling polar cap F -region patches using time varying convection, *Geophys. Res. Lett.*, **20**, 1783, 1993.
- Sojka, J. J., et al., Driving a physical ionospheric model with a magnetospheric MHD model, *J. Geophys. Res.*, **102**, 22,209, 1997.
- Tsunoda, R. T., High-latitude F region irregularities: A review and synthesis, *Rev. Geophys.*, **26**, 719, 1988.
- Weber, E. J., et al., F layer ionization patches in the polar cap, *J. Geophys. Res.*, **89**, 1683, 1984.
- Weber, E. J., et al., Polar cap F patches: Structure and dynamics, *J. Geophys. Res.*, **91**, 12,121, 1986.

N. A. Gondarenko and P. N. Guzdar, IREAP, University of Maryland, College Park, MD 20742, USA. (natalia@glue.umd.edu; guzdar@glue.umd.edu)

J. J. Sojka and M. David, CASS, Utah State University, Logan, UT 20742, USA. (jsojka@cass.usu.edu; mdavid@cass.usu.edu)